JOURNAL OF MATERIALS SCIENCE 30 (1995) 607–614

# Vapour-phase reduction and the synthesis of boron-based ceramic phases

## Part I *The phase equilibria in the B–C–N–O system*

S. J. YOON*, A. JHA
*Department of Materials Technology, Brunel University, Kingston Lane, Uxbridge, Middlesex, UB8 3PH, UK*

Thermodynamic calculations have been performed to establish the partial pressure relationships between the gaseous species BO and CO at an isotherm during the reduction–nitridation of boric anhydride. This relationship enables us to establish the condition for the formation of boron nitride ceramic phase by selecting a suitable nitriding atmosphere. Relevant Gibbs free-energy equations have also been considered for establishing the phase equilibrium relationships over a wide range of temperature in the B–C–N–O system. The importance of BO gas formation and its subsequent reduction to BN is also discussed.

## 1. Introduction

Boron nitride, also known as white graphite, is a stable high-temperature ceramic phase that has found a diversified range of use as engineering materials. Some of the important applications are as crucibles for molten metal and glass handling, components for high-temperature electric furnaces, in the nuclear industry as low-neutron cross-section material, and in tribological applications. The ceramic nitride, as its name suggests, is isomorphous and isoelectronic with graphite and has a hexagonal (h-BN) crystal structure that differs marginally with the graphitic structure. As compared in Fig. 1a and b, the h-BN structure has planar six-member rings stacked directly on top of each other. Each boron atom has a nitrogen-atom neighbour both within the layers and across the two layers. In the graphitic carbon structure, however, the carbon atoms in the adjacent layers are offset. The intraplanar bonding between the boron and nitrogen atoms is predominantly covalent with a considerably large peak phonon-energy at 1370 $cm^{-1}$ wavenumber which corresponds to (B–N stretching) [1], the magnitude of the wavenumber being an indicator of the strength of the covalent B–N bonds. Consequently, h-BN phase is one of the highest melting point materials, second only to graphite (in the absence of a nitrogen atmosphere the material tends to decompose). The interplanar bonds, on the other hand, are of weak Van der Waals type. The two types of widely different bonding explain the reasons for anisotropic electrical, mechanical and thermal properties of hexagonal boron nitride and graphitic carbon. The latter is manifested in the solid lubricating properties of this material, as also observed in the case of synthetic graphite powder. The covalent bonding between the nitrogen and boron atoms contributes to the low thermal expansion coefficient and moderately high hardness. The ceramic material is also known to have a high thermal conductivity which makes it favourable as a promising electronic substrate material. The relative softness, arising from Van der Waals bonding, also aids easier machining of this material as compared with diamond. Table I, shown below, presents some important engineering properties of h-BN and compares them with the properties of the diamond cubic form of BN.

The crystal structures of two metastable forms of stable h-BN differ considerably. The ever-elusive sphaleritic structure (c-BN), commonly known as the hard diamond form of boron nitride, has a diamond-cubic structure and resembles the properties of carbon diamond, whereas the wurtzite form (w-BN) has a hexagonal structure with both $sp^2$ and $sp^3$ hybridized bonds. In the cubic form, the B–N bond is $sp^3$ hybridized and the lower $sp^2$ state is the feature of graphitic structure. On this basis, the wurtzite form is considered as an intermediate "distorted" structure of h-BN while transforming to c-BN. W-BN is also known as the "hexagonal diamond" and its properties represent the two hybridized structures mentioned above. The crystal structures of w-BN and c-BN are shown in Fig. 1c and d, respectively.

A wide variety of boron- and nitrogen-based reagents has been used and tried for the preparation of h-BN phase via chemical methods. Gmelin's Handbook [2] and Ullmann's Encyclopedia [3] describe several methods for the synthesis of h-BN phase. The more recent ceramic text book written by Segal [4]

* *Present address*: Research Laboratories, POSCO (Pohang Iron and Steel Co. Ltd.), Korea.

0022–2461 

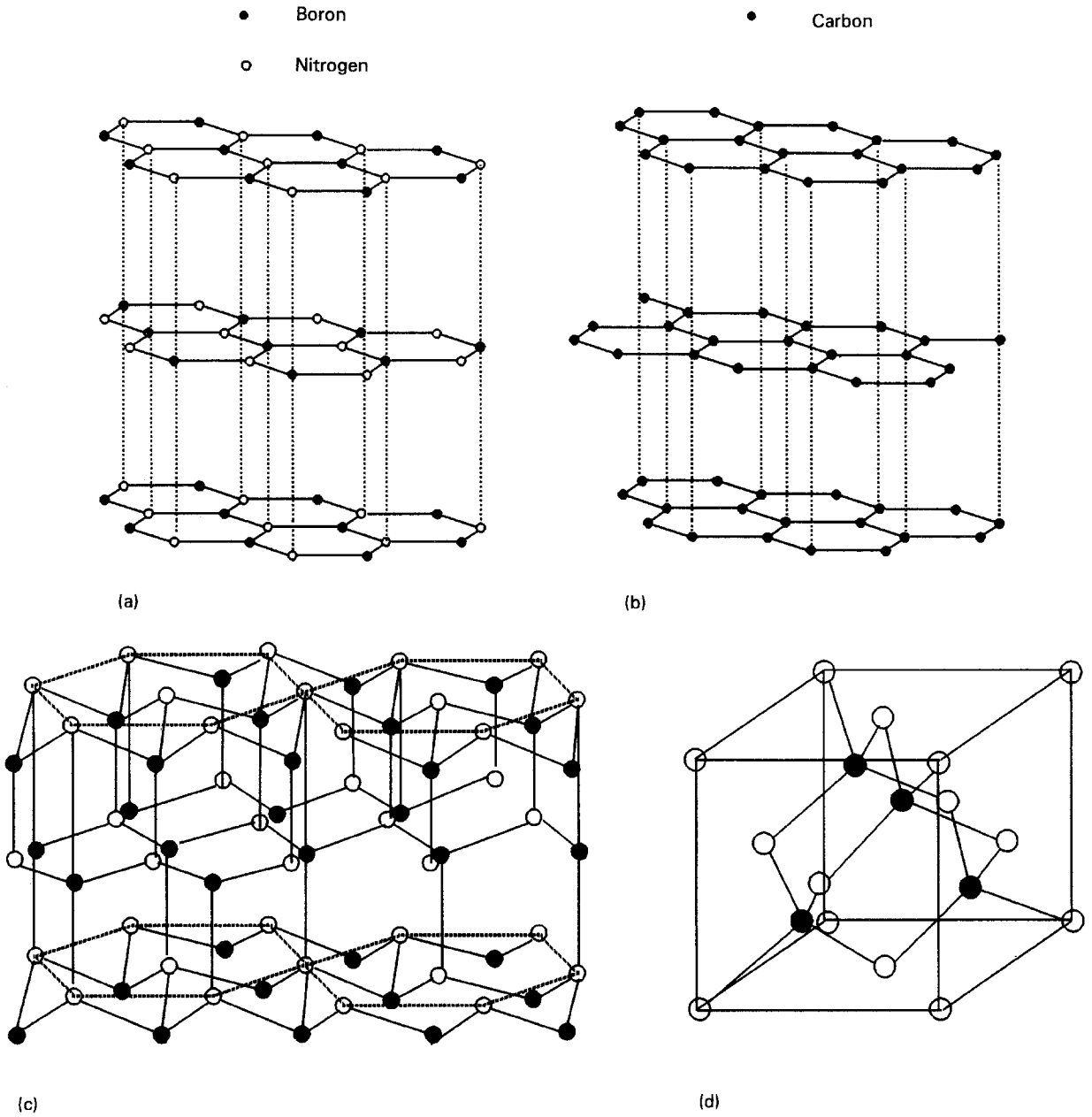


*Figure 1* Crystal structures of (a) hexagonal boron nitride (h-BN), (b) graphite, (c) wurtzite-type boron nitride (w-BN), (d) sphalerite-type boron nitride (c-BN).

TABLE I Comparison of properties of h-BN and c-BN [2, 3]

| Properties | h-BN | c-BN |
|---|---|---|
| Lattice parameters (nm) | $a = 0.2504$, $c = 0.6661$ | $a = 0.36157 \pm 0.0001$ |
| Density ($kg\,m^{-3}$) | 2270 (theoretical) | 3488 |
| Melting point (K) | 2600 (decomposition) | – |
| Specific heat ($J\,mol^{-1}\,K^{-1}$) | 17.460 | – |
| Thermal expansion ($K^{-1}$) | $41 \times 10^{-6}$ ($a$-axis), $-2.3 \times 10^{-6}$ ($c$-axis) | – |
| Thermal conductivity ($J\,m^{-1}\,s^{-1}\,K^{-1}$) | 15 ($a$-axis) 29 ($c$-axis) | – |
| Electrical resistivity ($\Omega$ cm) | $\sim 10^{13}$ | – |
| Dielectric constant, $e$ | 4.0–4.3 | – |
| Dielectric loss, tan$\delta$ | 0.0005 ($10^{10}$ c/s) | – |
| Hardness (GPa) | – | 60–70 |
| Young's modulus (GPa) | 32 (HIP h-BN) at 298 K | – |

also cites several methods for the synthesis of hexagonal BN. Typical examples are: pyrolytic boron nitride, carbothermic reduction of boric anhydride, nitridation of boron metal, reaction of either metal borides or $B_2O_3$ with ammonia. An alternative method for the production of BN advanced ceramic material utilizes the vapour deposition techniques such as the chemical vapour decomposition synthesis of $BCl_3$ gas in an atmosphere of ammonia leading to the formation of h-BN or amorphous form of BN (a-BN). The polymer

TABLE II A summary of reactions for the synthesis of hexagonal boron nitride

| Reaction | Operational temperature (K) |
|---|---|
| (1) $B_2O_3 + NH_3 = 2BN + 3H_2O$ | > 1173 |
| (2) $B_2O_3 + CO(NH_2)_2 = 2BN + CO_2 + 2H_2O$ | > 1773 |
| (3) $B + \frac{1}{2}N_2 = BN$ | > 1473 |
| (4) $B_2O_3 + 3C + N_2 = 2BN + 3CO$ | > 1773 |
| (5) $3CaB_2 + B_2O_3 + 10N_2 = 20BN + 3CaO$ | > 1473 |
| (6) $KBH_4 + NH_4Cl = BN + KCl + 4H_2$ | > 1173 |

pyrolysis routes are also a competitive route for BN synthesis. Neither of the above chemical processes, however, is capable of producing the high-pressure forms of boron nitride. The chemical reactions involved in various synthesis techniques for h-BN are summarized in Table II. This table includes the operational temperatures in absolute scale (K) estimated from the equilibrium thermodynamic calculations. For this, the approximated standard Gibbs free-energy change, $\Delta G^\circ$, for each chemical reaction, shown in Table II, was calculated from the data table compiled elsewhere [5]. The estimated temperature for each process is the minimum required for the synthesis of BN. For example, the $CO(NH_2)_2$ gaseous species was considered as a mixture of CO, $H_2$ and $NH_3$, because the standard Gibbs free energy of formation of this species is not known.

The price of commercially available BN ceramic powders is an important factor in determining the overall manufacturing cost of a ceramic engineering component. Reduction of oxides with carbon for the synthesis of a range of ceramic powders has proved to be an economically viable route with the recent commencement of pilot production of silicon and aluminium nitrides and boron carbide [6]. In the present series of articles on the "synthesis of boron-based ceramic powders", we have investigated the mechanism of the reduction of boric anhydride to boron nitride and carbide phases in the presence of carbon. In addition to the synthesis of boron-based compounds, we have also studied the simultaneous reduction of $TiO_2$ and $B_2O_3$ in the presence of carbon to $TiB_2$ and related ceramic and metal-matrix composite powder admixtures. The mechanism of formation of vapour phase species namely, $B_2O_3$ and BO gases, is of paramount significance in the reduction of oxide to relevant ceramic phase and, their presence in the reaction chamber is also known to determine the rate of reduction of $TiO_2$ to $TiB_2$ via carbothermic reduction of titania ($TiO_2$) and $B_2O_3$ powder mixtures. The transport mechanism of these reactive vapours and their subsequent conversion either to a required ceramic phase or to a ceramic phase mixture is the main principle adopted in the present investigation. This is discussed in four different parts. Part I of the present investigation covers the aspects of the phase equilibria in the B–N–C–O system and the calculation of thermodynamic equilibrium partial pressures of gaseous species for the synthesis of boron nitride phase. In Part II of the series, the mechanism of boron nitride synthesis reaction is discussed, together with a detailed analysis of the resultant microstructure of the nitride phase. In this context, the role of sub-oxide gaseous species during the nitriding reaction is particularly explained. In this section, the microstructural variations observed as a result of controlling the parameters of the carbothermic reduction process is compared with the structure of ceramic powder obtained from other routes. Part III will cover the aspects of the thermodynamic stability of the boron carbide phase and its microstructure. We have also reviewed the kinetics of boron carbide synthesis reaction and compare the results of kinetic analysis with the data obtained in the present investigation, Relevant chemical reaction model equations are derived and the predicted reaction rates are reported as a function of the temperature. The results of structural analysis will also be presented with a concluding note on the diversity of carbothermic reduction process in comparison to conventional arc furnace and magnesium-metal reduction process. Finally, Part IV will cover the aspects of the synthesis of titanium diboride via carbothermic reduction technique and, the results from the calculated phase equilibria, reaction rate and crystal growth kinetics and microstructure of the phases produced are discussed.

## 2. Thermodynamic aspects of the nitriding reaction

The phase equilibrium diagrams in the B–N–C–O system are important for determining the conditions for the synthesis of boron nitride and carbide phases. In the current literature, there is a lack of such information. However, relationships between the partial pressures of dominant gaseous species such as $B_2O_3$ and BO can be readily established by deriving the relevant free-energy functions in the B–N–C–O system. Several such examples are discussed below in order to determine the conditions for the reduction of boric anhydride to BN and $B_4C$ phases.

### 2.1. Vaporization of boric anhydride above its melting point

Boric anhydride ($B_2O_3$) at temperatures higher than its melting point (723 K) begins to evaporate; the vapour pressure of the gaseous phase was measured at different temperatures and compiled elsewhere [3]. Before we consider the thermodynamic aspects of the boric anhydride reduction–nitridation reaction, it is important to derive the free-energy equation for the vaporization of the boric anhydride liquid from the measured vapour pressure data. The vaporization reaction of $B_2O_3$ is defined as

$$B_2O_{3(liq)} = B_2O_{3(gas)} \quad (1)$$

for which the value of standard Gibbs free energy, $\Delta G = \Delta H - T\Delta S$, can be expressed in terms of the equilibrium constant

$$K_1 = \exp(-\Delta G_1/RT) = P_{B_2O_3(g)}/a_{B_2O_3(l)} \quad (2)$$

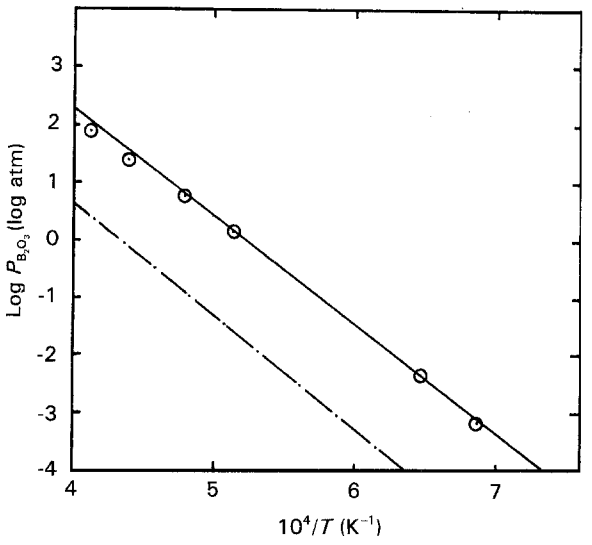


*Figure 2* A comparison of log $P_{B_2O_3}$ versus $1/T$ relationships for the vaporization of boric anhydride ($B_2O_3$). (– · –) from [7], $\Delta H$ = 362 670 J, $\Delta S$ = 155.7 J K$^{-1}$; (—⊙—) from [3], $\Delta H$ = 359 995 J, $\Delta S$ = 186.2 J K$^{-1}$.

Here $P$ and $a$ are the partial pressure and thermodynamic activity of the species respectively, under consideration. The vapour pressure of $B_2O_3$ gas was measured above pure boric anhydride liquid for which $a_{B_2O_3} = 1$ leading to

$$K_1 = \exp(-\Delta G_1/RT) = P_{B_2O_{3(g)}} \quad (3)$$

which can be written in terms of the enthalpy, $\Delta H_1$, and entropy, $\Delta S_1$, of the vaporization reaction. Therefore, Equation 3 can also be expressed as

$$\ln K_1 = -\Delta H_1/RT + \Delta S_1/R = \ln[P_{B_2O_{3(g)}}] \quad (4)$$

By constructing a straight line graphical relationship between $\ln[P_{B_2O_{3(g)}}]$ and $1/T$, the values of slope and intercept can be readily evaluated which will then yield the values of enthalpy and entropy of vaporization reaction in the temperature range shown in Fig. 2. The derived values of slope and intercept yielded the temperature dependence of the standard Gibbs free-energy change for the vaporization of boric anhydride in the temperature range 1450–2420 K, which is equal to $\Delta G = 359\,995 - 186.2T$ J mol$^{-1}$. The boiling point of $B_2O_3$ liquid is therefore 1933 K at which $P_{B_2O_3}$ is 1 atm. The derived values of $\Delta H$ and $\Delta S$ differ with the reported values in the thermodynamic data compilation in [7]. From data compilation, the measured value of boiling point of boric anhydride is 2329 K and the entropy of vaporization of liquid phase is 155.7 J mol$^{-1}$ K$^{-1}$. This yields the value of the enthalpy of vaporization which is equal to 362 670 J/mol $B_2O_3$. The vapour pressures of $B_2O_3$ at different temperatures, reported by Knacke *et al.* [7], are compared in Fig. 2. The two sets of data differ significantly and this is likely to have arisen due to the presence of moisture in the $B_2O_3$. The presence of moisture in $B_2O_3$ is known to enhance its rate of vaporization. In the present text, however, the measured results [3], shown in Fig. 2, have been used to perform the phase equilibria calculations. This option was exercised because in spite of handling $B_2O_3$ powders inside a dry glove box, the avoidance of moisture absorption during pellet preparation was proved to be an insurmountably difficult task.

## 2.2. Formation of sub-oxide gaseous species under reducting conditions

Boric anhydride, like $SiO_2$ and $Al_2O_3$, has a tendency to decompose at elevated temperatures to a sub-oxide species, namely boron monoxide (BO). This gas can form either from liquid or from gaseous boric anhydride. The reaction considered below

$$B_2O_3(\text{liq}) \text{ or } (\text{gas}) = 2BO_{(g)} + \tfrac{1}{2}O_{2(g)} \quad (5)$$

is thermodynamically less feasible. The values of standard Gibbs free-energy change for the formation of BO gas from liquid and gaseous boric anhydride are 1221 820 – 387.8$T$ J and 861 825 – 201.6$T$ J, respectively, and, the corresponding equilibrium temperatures are 3151 and 4275 K. These two equilibrium temperatures signify that the values of $K$ for reduction reactions are unity, i.e. $K_5 = (P_{BO})^2 \cdot (P_{O_2})^{1/2} = 1$. All thermodynamic calculations in this text have been performed by using the data compilation in [5]. From the sub-oxide formation reaction in Equation 5, it is apparent that provided the partial pressure of oxygen gas ($P_{O_2}$) is lower than the equilibrium partial pressure in the reaction chamber, the reaction equilibrium will shift in the forward direction. For example, at $T$ = 1573 K, the value of $P_{O_2}$ should be at least lower than $6.7 \times 10^{-37}$ atm which is the equilibrium partial pressure of oxygen for $B_2O_3$ (g) = 2BO(g) + $\frac{1}{2}O_2$(g) reaction. Such a low pressure is difficult to achieve in practice; therefore, an alternative means to lower the equilibrium temperature, $T_{eqm}$, and the oxygen partial pressure for Reaction 5 is to form a stable product gas such as CO. This can be achieved by the use of carbon. From Table III, note that the use of CO as a reducing gas leading to the formation of $CO_2$ as a product gas does not thermodynamically favour the sub-oxide formation reaction. The estimated equilibrium temperatures rise sharply due to the lower stability of $CO_2$ product gas than CO at elevated temperatures.

The calculated values of $T_{eqm}$ in Table III point out that in order to promote the formation of the sub-oxide gaseous species at a practically accessible temperature, the presence of carbon is essential. $B_2O_3$ gas will similarly convert into BO gas at temperatures above 2600 K. The reactions summarized in Table III are called "the BO generation reaction". The equilibrium constants, for example, $B_2O_{3(l)} + C_{(gr)} = 2BO_{(g)} + CO_{(g)}$ reaction is $K_{6a}$ and is equal to a product

$$K_{6a} = (P_{BO})^2 \cdot P_{CO} \quad (6a)$$

whereas with CO the relationship is

$$K_{6b} = (P_{BO})^2 \cdot P_{CO_2}/P_{CO} \quad (6b)$$

In Equations 6a and b, we have considered the pure liquid boric anhydride and graphitic carbon as the comparative thermodynamic standard states and,

TABLE III Values of standard Gibbs free-energy change and equilibrium temperatures for the formation of BO gas under reducing conditions

| Reaction | $T_{eqm}$ (K) | $\Delta G = \Delta H - T\Delta S$(J) |
|---|---|---|
| (a) $B_2O_{3(l)} + C_{(gr)} = 2BO_{(g)} + CO_{(g)}$ | 2338 | $1\,106\,844 - 473.4\,T$ |
| (b) $B_2O_{3(l)} + CO_{(g)} = 2BO_{(g)} + CO_{2(g)}$ | 3120 | $940\,730 - 301.5\,T$ |
| (c) $B_2O_{3(g)} + C_{(gr)} = 2BO_{(g)} + CO_{(g)}$ | 2600 | $747\,380 - 287.4\,T$ |
| (d) $B_2O_{3(g)} + CO_{(g)} = 2BO_{(g)} + CO_{2(g)}$ | 5038 | $580\,735 - 115.3\,T$ |

TABLE IV Values of standard Gibbs free-energy change for the reduction-nitridation of BO gas

| Reaction | $\Delta G = \Delta H - T\Delta S$(J) |
|---|---|
| (a) $BO_{(g)} + C_{(gr)} + \frac{1}{2}N_{2(g)} = BN_{(hex)} + CO_{(g)}$ | $-361\,420 + 90.7\,T$ |
| (b) $BO_{(g)} + C_{(gr)} + NH_{3(g)} = BN_{(hex)} + CO_{(g)} + 1.5H_{2(g)}$ | $-307\,633 - 25.9\,T$ |
| (c) $BO_{(g)} + CO_{(g)} + \frac{1}{2}N_{2(g)} = BN_{(hex)} + CO_{2(g)}$ | $-527\,938 + 261.8\,T$ |
| (d) $BO_{(g)} + CO_{(g)} + NH_{3(g)} = BN_{(hex)} + CO_{2(g)} + 1.5H_{2(g)}$ | $-474\,190 + 145.2\,T$ |

hence both $a_{B_2O_3}$ and $a_C$, by definition, reduce to a value of unity. For the reduction of $B_2O_3$ gaseous phase, the relationships shown in Equations 6a and b should then include the partial pressure of $B_2O_3$ gas in the denominator. Once the BO gas forms at elevated temperatures, it can be converted either to BN or to a boron carbide ($B_4C$) phase.

## 2.3. The reduction–nitridation of BO gas

The formation of BN can take place in the presence of a nitriding atmosphere either with nitrogen or with ammonia gas. For the synthesis of BN, the equilibria in the presence of nitrogen and ammonia gaseous atmospheres can then be expressed as

$$BO_{(g)} + C_{(gr)} + \tfrac{1}{2}N_{2(g)} = BN_{(hex)} + CO_{(g)} \quad (7a)$$

$$BO_{(g)} + C_{(gr)} + NH_{3(g)} = BN_{(hex)} + CO_{(g)} + 1.5H_{2(g)} \quad (7b)$$

The derived values of the standard Gibbs free-energy change for these two nitriding reactions are shown in Table IV for which the equilibrium constants $K_{7a}$ and $K_{7b}$ are

$$K_{7a} = \frac{P_{CO} \cdot 1}{P_{BO} \cdot (P_{N_2})^{1/2}} \quad (8a)$$

$$K_{7b} = \frac{P_{CO} \cdot (P_{H_2})^{1.5}}{P_{BO} \cdot P_{NH_3}} \quad (8b)$$

For comparative purposes, relevant equilibria for the formation of hexagonal boron nitride with CO as a reducing agent in the presence of nitrogen and ammonia are also considered below.

$$BO_{(g)} + CO_{(g)} + \tfrac{1}{2}N_{2(g)} = BN_{(hex)} + CO_{2(g)} \quad (9a)$$

$$BO_{(g)} + CO_{(g)} + NH_{3(g)} = BN_{(hex)} + CO_{2(g)} + 1.5H_{2(g)} \quad (9b)$$

The equilibrium constant relationships for the nitriding reactions with CO can be derived in a similar way as shown above in Equation 8a and b. The values of standard Gibbs free energy for Reactions 7a and b, 9a and b are summarized in Table IV. The chemical reactions summarized in Table IV are called "the consumption of BO gas" and their equilibrium constant relationships mathematically differ from that of the generation reactions. The overall reduction–nitridation reactions are the sums of BO generation reaction (cf. Table III) and the corresponding consumption reactions of BO during nitridation (cf. Table IV). Two particular examples of nitridation, one with nitrogen gas and the other with ammonia are discussed below

$$B_2O_{3(l)} + 3C_{(gr)} + N_{2(g)} = 2BN_{(hex)} + 3CO_{(g)} \quad (10a)$$

$$\Delta G_{10a} = 384\,537 - 292.2\,T\,J$$

and

$$B_2O_{3(l)} + 3C_{(gr)} + 2NH_{3(g)} = 2BN_{(hex)} + 3CO_{(g)} + 1.5H_{2(g)} \quad (10b)$$

$$\Delta G_{10b} = 492\,109 - 525.4\,T\,J$$

The equilibrium for these two reactions will shift in the forward direction above 1316 and 937 K, respectively. The lower equilibrium temperature in Reaction 10b is possible due to higher nitriding potential of ammonia gas than pure nitrogen. When ammonia decomposes, the partial pressure of nitrogen above the equilibrium temperature could exceed well above 1 atm. Furthermore while using ammonia gas, it is also important to consider the decomposition equilibrium constant relationship ($2NH_3 = N_2 + 3H_2$), i.e.

$$K_{NH_3} = P_{N_2}(P_{H_2})^3/(P_{NH_3})^2 \quad (11)$$

which suggests that if the partial pressure of $NH_3$ gas is fixed and $P_{H_2}$ is lowered in a $NH_3/H_2$ gas mixture such that the sum $P_{NH_3} + P_{H_2}$ changes only with $P_{H_2}$; then the partial pressure of nitrogen, as shown in Equation 11, will rise inversely with the cube power of $P_{H_2}$. This is particularly advantageous in manipulating the nitrogen chemical potential while synthesizing BN via Reaction 10b.

We also point out that while considering the equilibria related to the consumption of BO gas, the derived values of equilibrium temperatures from the free-energy equations do not reflect the true

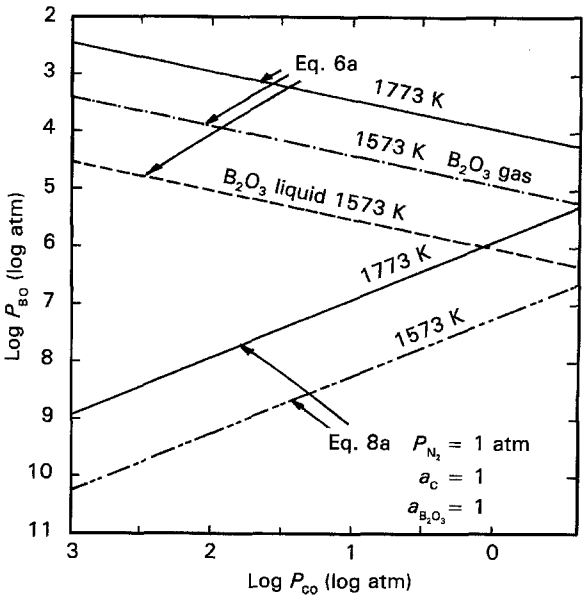


*Figure 3* Relationships drawn between the partial pressures of gases BO and CO at 1573 and 1773 K using Equations 6a and 8a. These two equations represent the BO generation and consumption reactions respectively. $P_{N_2} = 1$ atm, $a_c = 1$, $a_{B_2O_3} = 1$.

processing temperatures. This is because of the values and signs of $\Delta H$ and $\Delta S$ in the free-energy equation and, due to this much lower values of temperatures are predicted at which the BO gas is thermodynamically unstable. This aspect will become more apparent in the following section where the phase predominance area diagrams are established from the thermodynamic calculations.

From the equilibrium constant in Equations 6a and 8a, for example, we can establish relationships between BO and CO for a given nitrogen partial pressure or nitrogen potential and carbon activity at an isotherm. We find that for the sub-oxide gaseous phase generation reaction, the partial pressure of BO is inversely related to $P_{CO}$; whereas the partial pressure of BO is directly proportional to $P_{CO}$ for the consumption reaction. The relationships for both liquid and gaseous $B_2O_3$ are plotted in Fig. 3 for $P_{N_2} = 1$ atm. The presence of $B_2O_3$ gas enhances the corresponding vapour pressure of BO gas at a given CO partial pressure. This would mean that in practice the partial pressure of BO gas will rise approximately by an order of magnitude. However, by considering Equilibrium 7b, we find that equilibrium partial pressure of BO gas at $P_{NH_3} = 0.1$ and $P_{H_2} = 0.04$ atm, for example, drops substantially lower than when $P_{N_2} = 1$ atm. Evidently, the $P_{BO}$ partial pressure differential changes by nine orders of magnitude at 1573 K, and $P_{CO} = 0.1$ atm if nitrogen gas is replaced by ammonia as a nitriding agent. Such a large chemical potential difference will determine the driving force for the nucleation of ceramic phase and hence the particle size of BN will be expected to be dependent on this pressure differential because the rate of nucleation is dependent on this factor. From Fig. 3, it is also evident that as the equilibrium constant rises with increasing temperature, the $P_{BO}$–$P_{CO}$ line accordingly shifts to higher $P_{BO}$ values. In conclusion, it is apparent that the equilibrium partial pressure of BO in the reduction of $B_2O_3$ is always larger than that for the nitridation reaction. The temperature range selected in the calculated results shown in Fig. 3 also represents our experimental condition for the synthesis of hexagonal BN.

## 2.4. Phase equilibria in the B–N–C–O system

### *2.4.1. The reducing condition leading to the formation of boron carbide and nitride from boric anhydride*

The phase equilibrium diagrams in the B–N–C–O system were constructed by plotting $-RT\ln P_{N_2}$(kJ) against the reciprocal of the absolute temperature for the equilibrium relationships shown in Table V. We have assumed that the activity of carbon is unity and the total partial pressure of CO gas is 1 atm. From Fig. 4, we find that the univariants (a) and (c) listed in Table V, intersect each other at point B. This means that the phase field A′BD′ defines the stability region for boron carbide, whereas BN and $B_2O_3$ are stable above DBD′ and A′BD lines, respectively. The point B is the invariant point where three boron-containing condensed phases are in equilibrium with the gas-phase mixture of CO and nitrogen. We have also plotted CC′ univariant (reaction f in Table V) which defines the equilibrium between all boron compounds, carbon and nitrogen and CO gas mixture. As expected from the Gibbs phase rule, the line CC′ must go through point B. This is shown in Fig. 4. The line CC′ points out that the stability of boron anhydride has significantly changed to a higher $P_{N_2}$ value and this is only possible because $B_4C$ and $B_2O_3$ can combine to form BN phase. However, by plotting univariant (f) (i.e. line EE′ in Fig. 4), which is also concurrent at point B, the effect of $B_2O_3$ gas on the phase stability

TABLE V The values of the standard Gibbs free-energy change for the reduction condition of boron anhydride to BN and $B_4C$ and for the nitridation of boron carbide

| Reactions | $\Delta G°$(J) |
|---|---|
| (a) $B_2O_{3(l)} + N_2 + 3C = 2BN + 3CO$ | $384\,426 - 292\,T$ |
| (b) $B_2O_{3(l)} + B_4C + 2C + 3N_2 = 6BN + 3CO$ | $-576\,555 + 53\,T$ |
| (c) $B_4C + 2N_2 = 4BN + C$ | $-960\,981 + 345\,T$ |
| (d) $B_2O_{3(l)} + 7C = B_4C + CO$ | $1729\,833 - 929\,T$ |
| (e) $B_2O_{3(l)} + 2NH_3 = 2BN + 3H_2O$ | $92\,592 - 100\,T$ |
| (f) $B_2O_3(g) + B_4C + 2C + 3N_2 = 6BN + 3CO$ | $-936\,550 - 239.2\,T$ |

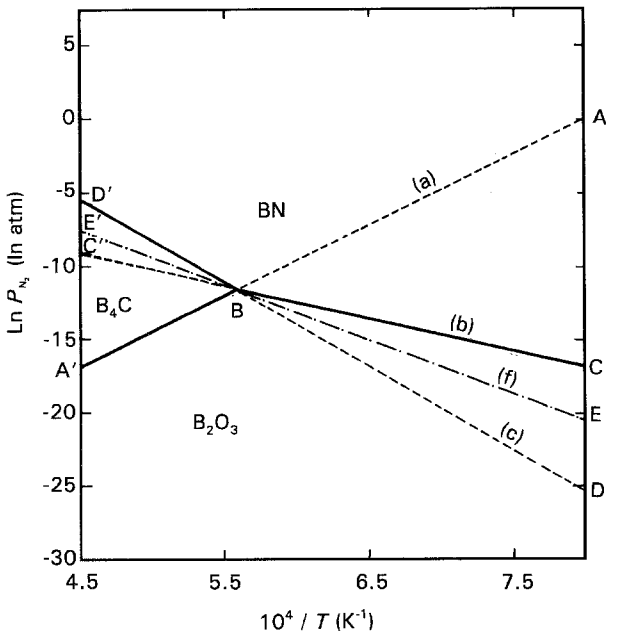


*Figure 4* Ln $P_{N_2}$ versus $1/T$ in the B–C–N–O system defining the regions of relative stability for $B_2O_3$, BN and $B_4C$ phases. Point "B" is an invariant point. $P_{CO} = 1$ atm. The univariants are defined in Table V and are designated (a), (b), (c), etc, in this figure and in the table.

can be recognized. Line EE′ reduces the phase stability area of $B_2O_3$ with the concomitant expansion of the BN phase field. The importance of the phase equilibrium calculation will become apparent in Part II of the present series, in which the experimental results are discussed. The new phase fields are as follows:

(a) above the curve A′BC, BN is stable;
(b) in the region A′BD′, $B_4C$ is stable;
(c) and below the curve A′BC, $B_2O_3$ is stable.

### 2.4.2. Equilibrium between metallic boron, $B_4C$, BN, carbon and the gas phase

An alternative method of establishing the phase relationships in the B–N–C–O system is to consider a set of independent chemical reactions that involves both the condensed phase and a gas-phase mixture composed of BO, CO and $N_2$. The equilibria we have considered are listed in Table VI. Additional reactions can also be considered but there are only five independent reactions relating to four boron-containing condensed phases, i.e. $B_2O_3$, B, $B_4C$ and BN. The other two dependent equilibria (F) and (G) are also shown in Table VI. Once the necessary equations are defined, the univariants (log $P_{BO}$ versus $T$) curves can be constructed by arbitrarily fixing the partial pressures of CO and $N_2$ gases. The total pressure is 1 atm and the thermodynamic activity of carbon is unity. The partial pressure of CO in all reactions in Table VI is 1 atm, except in Reaction (A) where we have arbitrarily fixed the partial pressure of nitrogen gas to 0.25 atm such that $P_{CO}/(P_{N_2})^{1/2} = 1$. This is to simplify the calculation of univariants described above. In Fig. 5, points a, b, c and d are the invariant points between two boron-containing condensed phases, one of which may be metastable, carbon and a gas mixture. At these points, the condensed phases are in equilibrium with CO and $N_2$ gas mixture. Owing to the metastability of one of the boron-containing phases, the thermodynamically unstable regime of BO gas is possible to define, as shown in Fig. 5.

For a complete representation of the B–C–O phase equilibria, Reactions (B)–(F) should be considered. The invariant point a determines the stability of BN

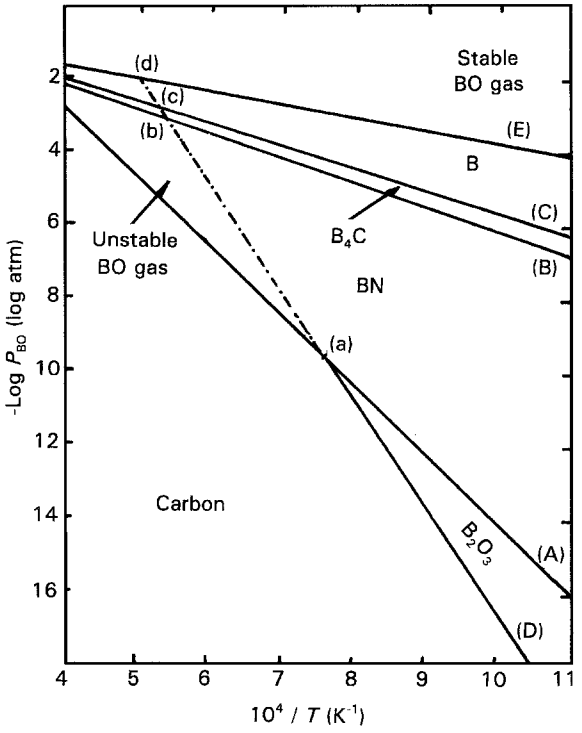


*Figure 5* Log $P_{BO}$ versus $1/T$ in the B–C–N–O system. The regions of phase stability are uniquely defined and points a, b, c and d are invariant points. Capital letters designate reactions in Table VI. $a_c = 1$ and $P_{N_2} = 1$ atm.

TABLE VI Phase equilibria equations in the presence of BO gas

| Reaction | $\Delta G°$(J) |
|---|---|
| (A) $BO + \frac{1}{2}N_2 + C = BN + CO$ | $-361\,209 + 90.63\,T$ |
| (B) $4BO + 5C = B_4C + 4CO$ | $-484\,854 + 17.61\,T$ |
| (C) $BO + C = B + CO$ | $-110\,587 + 3.01\,T$ |
| (D) $B_2O_{3(l)} + C = 2BO + CO$ | $1106\,844 - 473.38\,T$ |
| (E) $B_4C + BO = 5B + CO$ | $-69\,082 - 2.55\,T$ |
| (F) $B_2O_{3(l)} + B_4C = 4B + 2BO + CO$ | $1152\,152 - 390.16\,T$ |
| (G) $B_2O_{3(l)} + B_4C + 2N_2 = 4BN + 2BO + CO$ | $145\,863 - 128.49\,T$ |

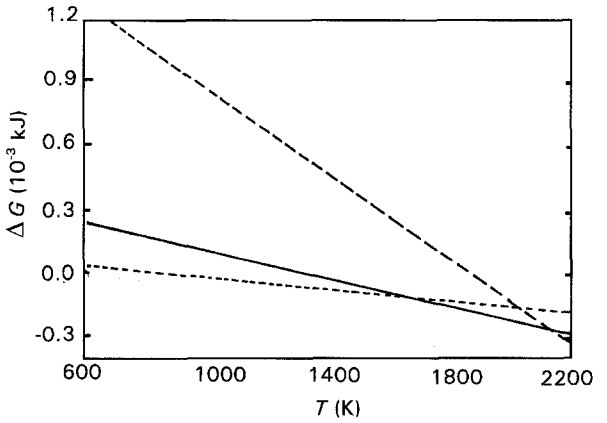


*Figure 6* A plot of standard Gibbs free-energy change, $\Delta G$, of BN or $B_4C$ against temperature, $T$, indicating the dominance of ammonia nitridation at lower temperatures. (——) BN ($N_2$), ( - - - ) $B_4C$, ( - - - ) BN ($NH_3$).

and boron anhydride phases over a wide range of temperature. Only above 1315 K, can BN crystals be thermodynamically stable and below this temperature $B_2O_3$ is a stable phase. Fig. 5 is an informative diagram and indicates the operational temperature range for the synthesis of ceramic and metal phases. This diagram also confirms why electric arc furnace operation yields $B_4C$ phase above 2473 K; this is because of the high-temperature stability of boron carbide phase.

In Fig. 6, the univariants for the carbothermic reduction and ammonia nitridation are plotted. The nitridation with ammonia has the lowest free energy in the low-temperature range and it will therefore favour the formation of BN which is also one of the ways for the synthesis for h-BN. At higher temperatures than 1500 K, nitridation with nitrogen gas becomes more stable and eventually above 2000 K boron carbide is the most stable phase. This is consistent with the above phase relationship shown in Figs 4 and 5.

## 3. Conclusion

The vapour pressure of $B_2O_3$ above its melting point is high and at the nitridation and reduction temperatures of boric anhydride, the vapour pressure changes by four orders of magnitude between 1423 and 1723 K. The value of enthalpy of vaporization of $B_2O_3$ from the data compilation in [7] is similar to the value reported in [3]. However, the entropy of vaporization appears to be dependent on the overall moisture content of $B_2O_3$.

The reduction–nitridation of either $B_2O_3$ liquid phase or gaseous phase proceeds via a two-step process. In the first step, $B_2O_3$ reduces to BO gas, called the "BO generation reaction" and, in the second stage, the sub-oxide gas is reduced in the presence of a nitriding gas. The presence of ammonia as a nitriding gas increases the partial pressure difference between the BO generation and reduction reactions. This pressure differential is an important factor in controlling the size of the ceramic phase.

The univariant diagrams in Figs 4–6 point out the regions of relative phase stability of BN, $B_4C$, $B_2O_3$ and metallic boron phases. Boron carbide is only stable at higher temperatures, and much larger partial pressures of BO gas is required to form this phase. On the other hand, boron nitride is stable over a large temperature range and at a relatively lower value of $P_{BO}$ than required for $B_4C$. Metallic boron, however, can only form well above the stability range of $B_4C$ as the equilibrium partial pressure of BO gas at a given temperature is higher than the value necessary for the stability of $B_4C$. This is evident from Fig. 5.

## Acknowledgements

The authors acknowledge the financial support from the Office of Overseas Research Students, UK.

## References

1. R. T. PAINE and C. K. NARULA, *Chem. Rev.* **90** (1990) 76.
2. A. MELLER, in "Gmelin Handbook of Inorganic Chemistry", 8th Edn, edited by K. Buschbeck (Springer, 1988) pp. 3–89
3. K. A. SCHWETZ and A. LIPP, in "Ullmann's Encyclopedia of Industrial Chemistry", Fifth Completely Revised Edn, Vol. A4, edited by W. Gerhartz (VCH, Munich, 1985) p. 295.
4. D. SEGAL, "Chemical Synthesis of Advanced Ceramic Materials", 1st Edn (Cambridge University Press, Cambridge, 1991) p. 89.
5. E. T. TURKDOGAN, "Physical Chemistry of High Temperature Technology" (Academic Press, 1980) pp. 5–24.
6. G. A. COCHRAN, C. L. CONNER, G. A. EISMAN, A. W. WEIMER, D. F. CARROLL, S. D. DUNMEAD and C. J. HWANG, in "Silicon Nitide 93", Proceedings of the International Conference on Silicon Nitride-Based Ceramics, Sttutgart, 4–6 October 1993, edited by M. J. Hoffmann, P. F. Becker and G. Petzow (Trans Tech Publications, Brookfield, Vermont) pp. 3–8.
7. O. KNACKE, O. KUBASCHEWSKI and K. HESSELMANN, "Thermochemical Properties of Inorganic Substances I", 2nd Edn (Springer, Berlin, 1991) p. 147.

*Received 19 May*
*and accepted 11 July 1994*